

PAPER • OPEN ACCESS

A robust estimation of the response of floating wind turbines through piecewise linearization

To cite this article: J Meng *et al* 2024 *J. Phys.: Conf. Ser.* **2647** 112007

View the [article online](#) for updates and enhancements.

You may also like

- [Objective identification of multiple large fire climatologies: an application to a Mediterranean ecosystem](#)
J Ruffault, V Moron, R M Trigo et al.
- [Design Optimization of Spar Floating Wind Turbines Considering Different Control Strategies](#)
John Marius Hegseth, Erin E. Bachynski and Joaquim R. R. A. Martins
- [Dual-ended readout of bismuth germanate to improve timing resolution in time-of-flight PET](#)
Sun Il Kwon, Emilie Roncali, Alberto Gola et al.



PRIMETM
PACIFIC RIM MEETING
ON ELECTROCHEMICAL
AND SOLID STATE SCIENCE
HONOLULU, HI
October 6-11, 2024

Joint International Meeting of
The Electrochemical Society of Japan (ECSJ)
The Korean Electrochemical Society (KECS)
The Electrochemical Society (ECS)

Early Registration Deadline:
September 3, 2024

**MAKE YOUR PLANS
NOW!**

A robust estimation of the response of floating wind turbines through piecewise linearization

J Meng¹, W Mostert¹, and M N Chatzis¹

¹ Department of Engineering Science, University of Oxford, Parks Road, OX1 3PJ Oxford, UK

E-mail: jiayao.meng@eng.ox.ac.uk

Abstract. Floating wind turbines (FWT) enable access to substantial wind resources in deep waters. They are hence anticipated to contribute significantly to the carbon-neutral target. Popular simulation tools for this relatively new offshore technology adopt the linear potential flow theory borrowed from the offshore oil and gas industry to evaluate the hydrodynamic forces, which are calculated around the equilibrium position of the platform. However, the compliance of the floating platform can potentially lead to large motions under combined wind and wave actions. To address this issue, the present work proposes a new piecewise linearization approach that can capture the nonlinearity by re-linearizing the wave-platform interaction system at instantaneous platform positions (operating points). A state-basis transformation algorithm is developed to ensure that the consistent physical basis is used across all operating points when calculating the fluid radiation force using the state-space representation. This new approach is implemented in a FWT Simulink model, and an open-source boundary element method code, Nemoh, is used to calculate the hydrodynamic force for the linearized wave-platform system at each operating point. Free vibration tests of a 5-MW ITIBarge FWT are examined to demonstrate the effectiveness of the piecewise linearization approach. The results obtained by this new approach are compared to the common practice of linearizing around the equilibrium, and the new approach is found to be able to conduct a fast and robust evaluation of the nonlinear hydrodynamics for FWTs.

1. Introduction

Around 80% of the offshore wind resource is located in waters deeper than 60 m, making FWTs the most economically viable technology to harness them. One of the major challenges faced by the floating wind industry is the fully-coupled dynamic analysis of FWTs, in which the floating foundation is a critical component. Although the relatively mature design and analysis methods for floating platforms in the oil and gas industry can be partially transferred to FWTs [1], the presence of the superstructure and large wind-induced platform motions can potentially affect the platform's hydrodynamic response which is challenging to model. Simplifications to the hydrodynamic modelling may lead to overly conservative platform design and thus high costs. In 2021, the representative Levelized cost of energy (LCoE) of floating wind was estimated as \$133/MWh, with the floating subsystem accounting for 36.5% of the total, compared to bottom-fixed offshore wind at \$78/MWh with its foundation only taking 6.7% [2]. The reliable and cost-effective design of FWTs is crucial in reducing floating wind cost and unlocking the substantial potential of offshore wind in the coming decades.

The prevalent analysis method for the FWT hydrodynamics calculation is a combination of linear potential flow theory and Morison's equation, which has been adopted by most FWT



simulation tools, e.g. OpenFAST [3] and HWAC2 [4]. By assuming small wave amplitude and small platform motions, this approach simplifies the highly nonlinear water-platform interaction problem to a linear problem around the equilibrium position. However, such assumptions would be violated under large waves and large wind-induced platform motions. In such cases, the validity of the prevalent method should be re-investigated. The OC5 project led by NREL [5] reported that 17 FWT simulation tools using linearization-based hydrodynamic calculation method consistently underpredicted low-frequency platform design loads compared to 1/50th-scale model test results for a 5-MW semisubmersible FWT. To accurately determine the nonlinear water-platform interaction effects, researchers have utilized high-fidelity methods such as Computational Fluid Dynamics (CFD) [6], Smoothed Particle Hydrodynamics [7], and fully-nonlinear potential flow theory [8], which capture instantaneous free surface and platform positions. Tran and Kim [9] observed large phase differences in platform motions between CFD and OpenFAST models for an operating 5-MW semisubmersible FWT under regular wave. Nematbakhsh et al [10] examined the CFD model of a 5-MW spar-type FWT and successfully captured large platform rotations (10°) and strong nonlinear effects, e.g. complete platform submergence and tether slacking under extreme sea states.

Despite the accuracy of high-fidelity models, their computational cost is significant [11]. The current design practice for FWTs involves thousands of simulations in the preliminary design and optimization phase [1]. This makes high-fidelity models more suitable for the final design verification [12]. However, using prevalent FWT hydrodynamic modelling tools in early phases can result in design candidates that are later found to be suboptimal and even infeasible [13]. To avoid costly design changes in the final stage, it is crucial to use reliable nonlinear models that capture the dominant platform dynamics with realistic computational costs [14]. Researchers have examined various methods to efficiently evaluate the nonlinear water-platform interaction effects. Al-Solihat and Nahon [15] proposed an analytical method to calculate nonlinear hydrostatic loads of a spar-type FWT. Chan et al. [16] investigated the 5-MW MIT/NREL TLP FWT by integrating the fluid-impulse theory with FAST, and calculated the hydro-mechanical forces over the instantaneous wetted body surface. The surge diffraction force obtained from their model was reported to be larger than that from FAST's linear HydroDyn code. Offline models that consider the body surface nonlinearity have been studied for wave energy converters (WEC) [17]. The hydrodynamic coefficients pre-calculated from a series of body positions are stored in a database, which is then used to interpolate for the hydrodynamic force at each time step using the instantaneous body motion. Clear differences in body responses were reported compared to experiment results. However, as the WEC is fully submerged, the conclusion should be re-investigated for FWTs.

In this conference paper, a piecewise linearization framework is proposed to evaluate the effects of the time-varying wetted body surface, and its implementation is examined in a Simulink FWT model. The framework utilizes an open-source BEM code, Nemoh, to update the hydrodynamic coefficients at each operating point. These coefficients are used to identify a state-space model to approximate the fluid-memory radiation force. The state-space model estimated through subspace identification algorithms at different operating point has different state basis, and thus cannot be directly pieced together. A state-basis conversion method is developed in this paper, which can effectively transform an unknown numerically selected state basis to the physical one that is not changing over the re-linearizations. Free-vibration tests of an example 5-MW ITI-Barge FWT model in Simulink is investigated to assess the proposed piecewise linearization framework, and to shed light on the nonlinear effects induced by the varying body-surface boundary condition.

2. Water-platform interaction modelling

Two right-handed coordinate systems are defined to describe the 3D movements of a FWT platform as well as the wave kinematics in an open sea of finite depth H (as shown in Fig.1). Let O be the Center of Gravity (CoG) when the FWT is in the static equilibrium position. The Cartesian coordinate system $OXYZ$ is earth-fixed, with the plane OXY parallel to the still water surface, OX pointing downwind, and OZ pointing upwards. The other coordinate system $O'X'Y'Z'$ is fixed on the platform and coincides with $OXYZ$ in the absence of perturbations. The translational displacement from O to O' in the surge, sway, and heave Degree of Freedom (DoF) is denoted as ξ_1, ξ_2, ξ_3 , respectively, and the rotation of roll, pitch and yaw DoF as ξ_4, ξ_5, ξ_6 , respectively. The Euler angle sequence is Cartesian $X \rightarrow$ rotated Y following the ξ_4 transformation \rightarrow rotated Z following the ξ_4 and ξ_5 transformations, as shown in Fig.1.

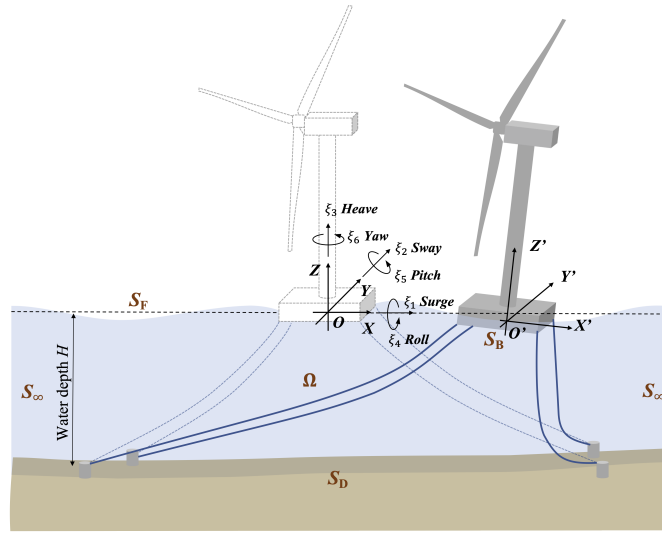


Figure 1: Coordinate system of a floating wind turbine. Only 6 platform DoFs are shown.

2.1. Nonlinear boundary value problem (BVP)

Ideal fluid (homogeneous, inviscid, and incompressible) without rotational motion and surface tension is assumed here, in which case the flow can be completely described by a velocity potential $\Phi(x, y, z, t)$ satisfying Laplace's equation. Φ can be determined given the combined nonlinear kinematic and dynamic boundary condition on the instantaneous free surface $S_F(t) : z = \eta(x, y, t)$, impermeability condition on the body surface $S_B(t)$ and sea bottom S_D , far-field condition on S_∞ , as well as initial conditions. These equations constitute the BVP of the water-platform interaction model and are summarized as follows:

$$\begin{cases} \nabla^2 \Phi = 0, & \mathbf{X} \in \Omega \\ \left(\frac{\partial}{\partial t} + \nabla \Phi \cdot \nabla \right) \left(\frac{\partial \Phi}{\partial t} + \frac{1}{2} \nabla \Phi \cdot \nabla \Phi + gz \right) = 0, & \mathbf{X} \in S_F(t) \\ \frac{\partial \Phi}{\partial \mathbf{n}} = \mathbf{V} \cdot \mathbf{n}, & \mathbf{X} \in S_B(t) \\ \nabla \Phi \cdot \mathbf{n} = 0, & \mathbf{X} \in S_D \\ \nabla \Phi < \infty, & \mathbf{X} \in S_\infty \\ \Phi(x, y, z, 0) = 0, \quad \frac{\partial \Phi(x, y, z, 0)}{\partial t} = 0, \end{cases} \quad (1)$$

where $\mathbf{X} = [x \ y \ z]^\top$ is the field point, $\nabla^2 = \frac{\partial^2}{\partial x^2} + \frac{\partial^2}{\partial y^2} + \frac{\partial^2}{\partial z^2}$, g the gravitational constant, $\mathbf{V}(t) = \dot{\boldsymbol{\xi}}(t)$ the body velocity, and \mathbf{n} the normal vector at body surface pointing out of fluid. The fluid pressure $p(x, y, z, t)$ can be obtained from Bernoulli's equation

$$p = -\rho \frac{\partial \Phi}{\partial t} - \frac{1}{2} \rho (\nabla \Phi)^2 - \rho g z, \quad (2)$$

where ρ is the fluid density.

2.2. Linearization of the BVP

The fully nonlinear dynamic and kinematic conditions on the time-varying free surface $\eta(x, y, t)$, as well as the coupling between fluid behavior and floating body dynamics, pose great difficulties in solving the BVP (Eq.1). By assuming small wave amplitudes relative to the wavelength, and small displacements and rotations of the platform relative to the platform's characteristic dimension, the nonlinear BVP can be simplified to a linear one, with the boundary conditions being satisfied on the still water level (\bar{S}_F) and mean wetted body surface (\bar{S}_B). This simplification enables the decomposition of Φ into an incident wave potential Φ_I , radiation potential Φ_R and diffraction potential Φ_D . Φ_R handles nonhomogeneous body surface boundary conditions, Φ_I is an exogenous input to the fluid-body system and Φ_D is used to cancel out the influence of Φ_I onto the body surface. The total velocity potential can be written as

$$\begin{aligned} \Phi(x, y, z, t) &= \Phi_R(x, y, z, t) + \Phi_I(x, y, z, t) + \Phi_D(x, y, z, t) \\ &= \Re \left\{ \frac{1}{2\pi} \int_{-\infty}^{\infty} \{ \bar{\mathbf{V}}(\omega) \cdot \boldsymbol{\phi}_R(x, y, z, \omega) + \bar{\eta}_o(\omega) [\phi_I(x, y, z, \omega) + \phi_D(x, y, z, \omega)] \} e^{i\omega t} d\omega \right\}, \end{aligned} \quad (3)$$

where $\boldsymbol{\phi}_R$ is the radiation wave potential vector corresponding to different platform DoFs, which is, however, independent of the platform velocity; ϕ_I, ϕ_D are the incident and diffraction wave potential, respectively, and they are independent of the wave elevation; $\bar{\mathbf{V}}(\omega), \bar{\eta}_o(\omega)$ are Fourier transform of the body velocity and wave amplitude at the projection of origin $\eta_o(t)$ onto the free surface, respectively. The governing equations of the linear BVP in the frequency domain can then be derived and summarized as:

$$\begin{cases} \nabla^2 \phi = 0, & \mathbf{X} \in \Omega \\ \frac{\partial \phi}{\partial z} - \frac{\omega^2}{g} \phi = 0, & \mathbf{X} \in \bar{S}_F : z = 0 \\ \frac{\partial \phi_R}{\partial \mathbf{n}} = \bar{\mathbf{n}}, \quad \frac{\partial (\phi_I + \phi_D)}{\partial \mathbf{n}} = 0, & \mathbf{X} \in \bar{S}_B \\ \frac{\partial \phi}{\partial z} = 0, & \mathbf{X} \in S_D : z = -H \\ \lim_{x \rightarrow \pm\infty} \left(\frac{\partial \phi}{\partial x} \mp ik\phi \right) = 0, \end{cases} \quad (4)$$

where $\bar{\mathbf{n}} = [\mathbf{n}; \mathbf{r} \times \mathbf{n}]$, \mathbf{r} is the position vector on the body surface. According to Airy's wave theory, the incident wave propagating along positive X direction takes the form

$$\phi_I(x, y, z, \omega) = \frac{ig}{\omega} \cdot \frac{\cosh[k(z+H)]}{\cosh(kH)} e^{ikx}, \quad (5)$$

where k is the wave number satisfying the dispersion relation

$$\omega^2 = gk \tanh(kH). \quad (6)$$

With the velocity potentials (Φ_I , Φ_R , and Φ_D), hydrodynamic pressure p can be obtained from Bernoulli's equation (Eq.2) with the high-order term $\frac{1}{2}\rho(\nabla\Phi)^2$ being neglected, and hydrodynamic forces acting on the body can be determined by integrating the pressure over body surface \bar{S}_B . Given these hydrodynamic forces, one can write the equations of motion (EoM) of the floating platform as a set of linear equations in the frequency domain:

$$\{-\omega^2 [\mathbf{M} + \boldsymbol{\lambda}(\omega)] + i\omega\boldsymbol{\mu}(\omega) + \mathbf{K}_{hs}\} \bar{\boldsymbol{\xi}}(\omega) = \bar{\eta}_o(\omega)\mathbf{F}_w(\omega) + \mathbf{F}_{b0} - \mathbf{G}, \quad (7)$$

where \mathbf{M} is the rigid-body mass of the platform, \mathbf{K}_{hs} the hydrostatic restoring stiffness, \mathbf{F}_{b0} the buoyancy force in the static equilibrium position which is balanced by platform weight \mathbf{G} , and $\boldsymbol{\lambda}$, $\boldsymbol{\mu}$, \mathbf{F}_w denotes the frequency-dependent added mass, radiation damping, wave excitation force transfer function, respectively:

$$\begin{aligned} \boldsymbol{\lambda}(\omega) &= \rho \iint_{\bar{S}_B} \bar{\mathbf{n}} [\phi_R^{Re}]^\top dS, \\ \boldsymbol{\mu}(\omega) &= -\rho\omega \iint_{\bar{S}_B} \bar{\mathbf{n}} [\phi_R^{Im}]^\top dS, \\ \mathbf{F}_w(\omega) &= -\rho i\omega \iint_{\bar{S}_B} (\phi_I + \phi_D) \bar{\mathbf{n}} dS, \end{aligned} \quad (8)$$

which can be calculated using Boundary Element Method (BEM) codes, e.g. Nemoh [18]. More details can be found in [22].

2.3. Linear time-domain analysis

To investigate the response of the system over time and integrate with other time-dependent subsystems, Cummins equation [19] is introduced to convert the frequency-domain equations (Eq.7) into a set of integro-differential equations with constant coefficients:

$$[\mathbf{M} + \boldsymbol{\lambda}(\infty)] \ddot{\boldsymbol{\xi}}(t) + \mathbf{F}_r(t) + \mathbf{K}_{hs}\boldsymbol{\xi}(t) = \mathbf{F}_{wt}(t) + \mathbf{F}_{b0} - \mathbf{G}, \quad (9)$$

$$\mathbf{F}_r(t) = \int_0^t \mathbf{k}(t - \tau) \dot{\boldsymbol{\xi}}(\tau) d\tau, \quad (10)$$

where $\boldsymbol{\lambda}(\infty) = \boldsymbol{\lambda}(\omega)|_{\omega \rightarrow \infty}$ is the infinite-frequency added mass, $\mathbf{k}(t)$ is the impulse response function representing fluid memory effect:

$$\mathbf{k}(t) = \frac{2}{\pi} \int_0^\infty \boldsymbol{\mu}(\omega) \cos(\omega t) d\omega, \quad (11)$$

and it is the Fourier transform of the frequency response function $\mathbf{K}(\omega)$ mapping from the platform velocity $\dot{\boldsymbol{\xi}}(t)$ to fluid-memory radiation force $\mathbf{F}_r(t)$:

$$\mathbf{K}(\omega) = \boldsymbol{\mu}(\omega) + j\omega [\boldsymbol{\lambda}(\omega) - \boldsymbol{\lambda}(\infty)]. \quad (12)$$

The calculation of the convolution integral $\mathbf{F}_r(t)$ at each time step is computationally expensive. To enhance efficiency, state-space representations have been proposed:

$$\begin{cases} \dot{\mathbf{x}}_r(t) = \mathbf{A}_r \mathbf{x}_r(t) + \mathbf{B}_r \dot{\boldsymbol{\xi}}(t) \\ \mathbf{F}_r(t) = \mathbf{C}_r \mathbf{x}_r(t) + \mathbf{D}_r \dot{\boldsymbol{\xi}}(t). \end{cases} \quad (13)$$

The state-space model can be identified either from the impulse response data $k_{mn}(t)$ (Eq.11) or frequency-response data $K_{mn}(\omega)$ (Eq.12) ($m, n = 1, 2, \dots, 6$) using subspace-based state-space identification (SSI) algorithms [20].

2.4. Piecewise linearization framework

The small platform motion assumption discussed in Section 2.2 breaks down when the platform undergoes large movements under winds and waves. To investigate the influence of the varying wetted body surface on platform dynamics, a new piecewise linearization approach is proposed in this work. In this preliminary study, the assumption of small wave amplitude is retained and the nonlinear free-surface boundary condition in Eq.1 is still linearized on $\bar{S}_F(z = 0)$. In contrast, the nonlinearity induced by the varying body surface boundary is estimated by re-linearizing the BVP at the platform position at time $t = NT_s$ ($N = 0, 1, 2, \dots$), where T_s is the time interval of executing a BEM code to solve the new BVP. The updated hydrodynamic coefficients $\boldsymbol{\lambda}(\omega)$, $\boldsymbol{\mu}(\omega)$ at n specified wave frequencies ω_d ($d = 1, 2, \dots, n$) obtained from the BEM code are then used to identify the state-space model $[\mathbf{A}_r, \mathbf{B}_r, \mathbf{C}_r, \mathbf{D}_r]$ representing the fluid-memory radiation force $\mathbf{F}_r(t)$. It should be noted that the identified state-space model Eq.13 is along a basis $\mathbf{x}_r(t)$, which is numerically chosen indirectly by the SSI algorithm, and hence is not consistent between the N -th and $N + 1$ -th re-linearization. It is crucial to convert them to the same basis otherwise erroneous radiation forces are resulted when re-linearization occurs. In this work, the algorithm proposed by Chatzis et al. [21] is modified to convert a state basis that is chosen by the SSI algorithm onto the physical one that is not changing over the re-linearizations. The physical basis is specified such that the state-space matrices in the physical coordinates have the following structure:

$$\mathbf{A}_r^p = \begin{bmatrix} \mathbf{0} & \mathbf{I} \\ \mathbf{A}_{21} & \mathbf{A}_{22} \end{bmatrix}, \mathbf{B}_r^p = \begin{bmatrix} \mathbf{0} \\ \mathbf{B}_2 \end{bmatrix}, \mathbf{C}_r^p = [\mathbf{I} \quad \mathbf{C}_2], \mathbf{D}_r^p = [\mathbf{D}]. \quad (14)$$

The physical state-space matrices $[\mathbf{A}_r^p, \mathbf{B}_r^p, \mathbf{C}_r^p, \mathbf{D}_r^p]$ are associated with the identified ones $[\mathbf{A}_r, \mathbf{B}_r, \mathbf{C}_r, \mathbf{D}_r]$ through a transformation matrix \mathbf{T} :

$$\mathbf{A}_r = \mathbf{T}^{-1} \mathbf{A}_r^p \mathbf{T}, \quad \mathbf{B}_r = \mathbf{T}^{-1} \mathbf{B}_r^p, \quad \mathbf{C}_r = \mathbf{C}_r^p \mathbf{T}, \quad \mathbf{D}_r = \mathbf{D}_r^p. \quad (15)$$

Given Eq.14 and $[\mathbf{A}_r, \mathbf{B}_r, \mathbf{C}_r, \mathbf{D}_r]$, one can find the solutions to the transformation matrix \mathbf{T} and the matrices of $[\mathbf{A}_r^p, \mathbf{B}_r^p, \mathbf{C}_r^p, \mathbf{D}_r^p]$. The radiation force \mathbf{F}_r calculated from the state-space model that is converted to the physical basis, as well as the updated $\boldsymbol{\lambda}(\infty)^{[N]}$, $\mathbf{K}_{hs}^{[N]}$ and $\mathbf{F}_b^{[N]}$ are subsequently incorporated into the following EoMs to solve the platform motion $\boldsymbol{\xi}, \dot{\boldsymbol{\xi}}, \ddot{\boldsymbol{\xi}}$, as well as the radiation states in the physical basis \mathbf{x}_r^p for the next time instant during $NT_s < t < (N+1)T_s$:

$$[\mathbf{M} + \boldsymbol{\lambda}(\infty)^{[N]}] \ddot{\boldsymbol{\xi}}(t) + \mathbf{F}_r(t) + \mathbf{K}_{hs}^{[N]} \int_{NT_s}^t \dot{\boldsymbol{\xi}}(t) dt = \mathbf{F}_{wt}(t) + \mathbf{F}_b^{[N]} - \mathbf{G}, \quad (16)$$

$$\begin{cases} \dot{\mathbf{x}}_r^p(t) = \mathbf{A}_r^{p[N]} \mathbf{x}_r^p(t) + \mathbf{B}_r^{p[N]} \dot{\boldsymbol{\xi}}(t) \\ \mathbf{F}_r(t) = \mathbf{C}_r^{p[N]} \mathbf{x}_r^p(t) + \mathbf{D}_r^{p[N]} \dot{\boldsymbol{\xi}}(t). \end{cases} \quad (17)$$

The flowchart of the proposed piecewise linearization framework is summarized in Figure 2.

3. Implementation of piecewise linearization framework for FWTs in Simulink

A FWT simulink model developed by the authors [22] is utilized in this work. The hub, nacelle, and floating platform that have relatively small internal deformation can be modeled as rigid bodies with lumped mass and inertia defined at their CoGs. The tower and blades are modelled as rigid in the present work. The focus of this conference paper is on evaluating the nonlinear water-platform interaction effects induced by the varying platform wetted surface. Consequently, the aerodynamics calculation and controller are switched off for the simulations, and no incident waves are exerted on the FWT ($\mathbf{F}_{wt}(t) = 0$ in Eq.16). The topology of the FWT model in Simulink is illustrated in Fig.3.

The piecewise linearization framework, as depicted in Figure 2, is implemented in the FWT Simulink model to evaluate the nonlinear hydrodynamic forces. The zero-order holds before

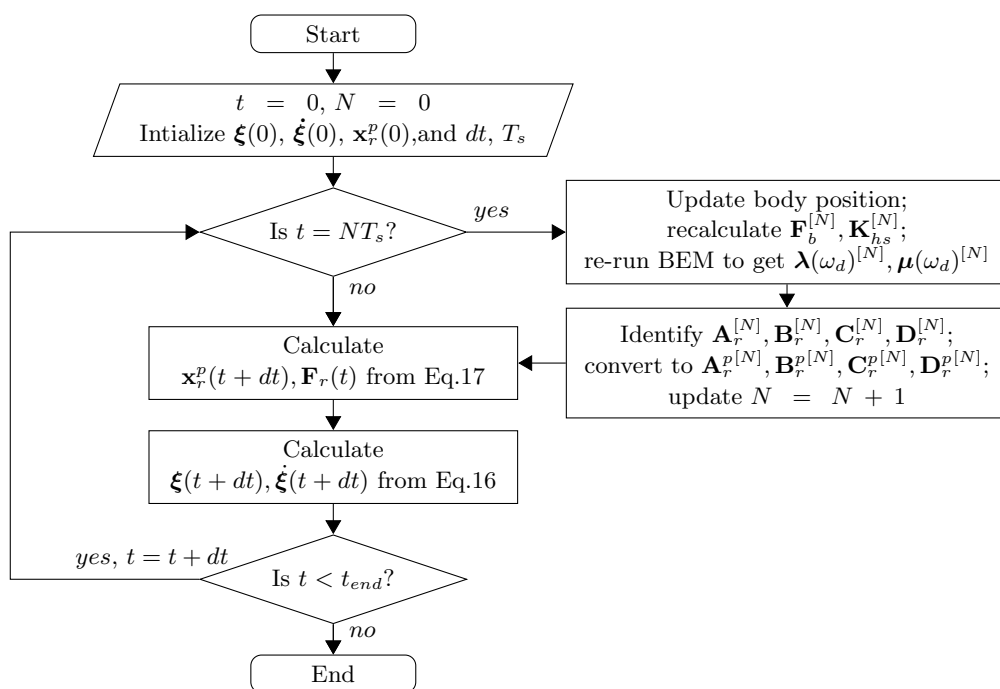


Figure 2: Flowchart of the piecewise linearization framework.

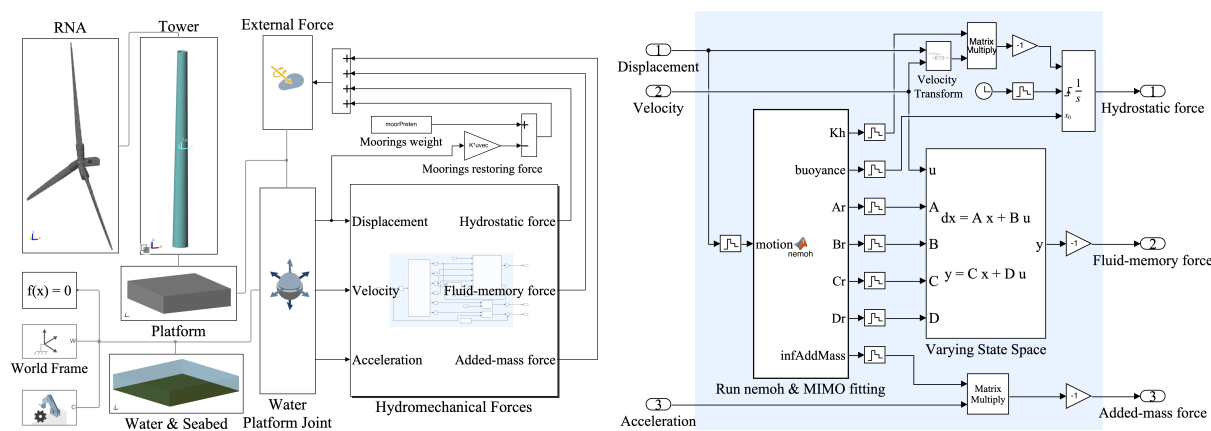


Figure 3: Topology of a floating wind turbine developed in MATLAB/Simulink environment.

and after the matlab function block are used to control the re-linearization every T_s . Upon the execution of N -th re-linearization, the wetted body surface is calculated based on the current platform displacements $\boldsymbol{\xi}(t = NT_s)$. The open-source BEM code, Nemoh, is called extrinsically in the matlab function block, which receives the geometry of the submerged surface and output the frequency-dependent hydrodynamic coefficients. The state-space matrices identified from these coefficients $\mathbf{A}_r^{[N]}, \mathbf{B}_r^{[N]}, \mathbf{C}_r^{[N]}, \mathbf{D}_r^{[N]}$ are then converted to those in the physical basis $\mathbf{A}_r^{p[N]}, \mathbf{B}_r^{p[N]}, \mathbf{C}_r^{p[N]}, \mathbf{D}_r^{p[N]}$ and are passed to the varying state-space block to calculate the fluid-memory radiation force. The updated infinite-frequency added mass $\boldsymbol{\lambda}(\infty)^{[N]}$ and hydrostatic stiffness $\mathbf{K}_{hs}^{[N]}$ are multiplied by the platform acceleration $\ddot{\boldsymbol{\xi}}(t)$ and the integration of $\dot{\boldsymbol{\xi}}(t)$, respectively, to compute the added-mass force and buoyancy increment. Additionally, the moorings' restoring effects are modeled using a stiffness matrix, which is multiplied by the

platform displacement $\xi(t)$ to obtain the restoring forces. The aforementioned forces, along with the weight of moorings and displaced water by the platform, are summed and applied to the 6-DoF water-platform joint, as shown in Figure 3. After building the full system and specifying initial conditions, the time-domain dynamic analysis can be conducted by solving the EoMs numerically using in-built ODE solvers in Simulink.

4. Example and discussions

An example of the 5-MW ITIBarge FWT [23] is taken to evaluate the piecewise linearization framework. The ITIBarge platform has a width of 40 m, length of 40 m, draft of 4 m and is floating on water with a depth of $H = 150$ m. The platform is moored with 8 catenary mooring lines. Their weight and restoring stiffness are obtained from the quasi-static mooring analysis code, MAP++ [24], and are imported in the Simulink model. To examine the effectiveness of the piecewise linearization framework in capturing the nonlinear water-platform interaction effects, a simple example of activating only the heave DoF of the Simulink FWT model is conducted.

A convergence test for the hydrodynamic frequency response data in heave DoF $\mathbf{K}_{3,3}(\omega)$ around the equilibrium position is conducted with 4 mesh numbers ranging from 200-1200. Quadrilateral meshes over the whole submerged body surface as well as the virtual water-plane lid are utilized. The frequency response data $\mathbf{K}_{3,3}$ calculated using different mesh numbers are compared in Figure 4a. A mesh number of 400 can accurately calculate $\mathbf{K}_{3,3}$ in just around 1 minute for 100 wave frequencies, making it an optimal choice for piecewise linearization simulations. It should be noted that the singularity at around 2.5 rad/s leads to scattered BVP solution and tends to yield large discrepancies for high-frequency results between different mesh resolutions. These issues can be effectively addressed by data preprocessing, which removes spikes around the singularity and sets lower weighting factors to high-frequency data. The processed frequency response data is used to estimate the state-space model $[\mathbf{A}_r, \mathbf{B}_r, \mathbf{C}_r, \mathbf{D}_r]$. As only one measurement, i.e. radiation force in heave, is provided, the state-space model that can be converted to the physical basis has the maximum of 2 states. The original Nemoh's frequency response data, processed Nemoh's data, and the estimated function calculated from the state-space model are compared in Figure 4b. As shown in Figure 4b, the estimated state-space model provides a robust approximation to the hydrodynamic radiation force of the platform. The state-basis conversion method described in Section 2.4 is demonstrated here. The originally identified state-space matrices are listed as follows:

$$\mathbf{A}_r = \begin{bmatrix} -0.44 & 1 \\ -0.32 & -0.44 \end{bmatrix}, \mathbf{B}_r = \begin{bmatrix} 0 \\ 2126.73 \end{bmatrix}, \mathbf{C}_r = [-1104.46 \quad 2736.59], \mathbf{D}_r = [0].$$

With the transformation matrix

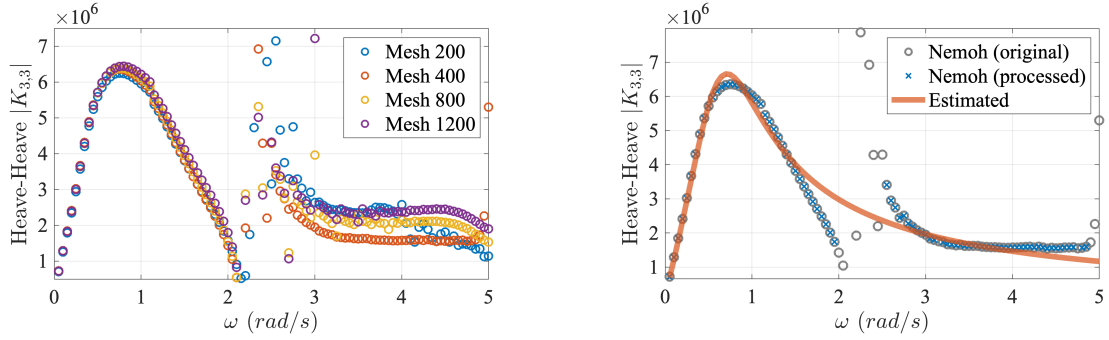
$$\mathbf{T} = \begin{bmatrix} 92.41 & 0 \\ -40.42 & 92.41 \end{bmatrix},$$

the state-space matrices with the physical basis can be obtained using Eq.15:

$$\mathbf{A}_r^p = \begin{bmatrix} 0 & 1 \\ -0.51 & -0.87 \end{bmatrix}, \mathbf{B}_r^p = \begin{bmatrix} 0 \\ 196538.88 \end{bmatrix}, \mathbf{C}_r^p = [1 \quad 29.61], \mathbf{D}_r^p = [0],$$

which has the same structure with Eq.14 as expected.

Free vibration tests are examined by releasing the FWT from an initial heave displacement of $\xi_3(0) = 2$ m with zero velocity. The platform responses simulated using different re-linearization time intervals T_s are compared in Figure 5a. The purely linear model responses simulated from both the Simulink model and OpenFAST (v3.2.1) are also shown, in which the hydrodynamic



(a) Frequency response data calculated by Nemoh with different total mesh numbers. (b) Identification results of the frequency response function for a mesh number of 400.

Figure 4: Convergence test of Nemoh in platform equilibrium position and identification results.

coefficients are calculated only once at the equilibrium position. It can be seen that the nonlinear simulation converges between $T_s = 0.1s$ and $0.05s$. The converged nonlinear results indicated that the heave response is different from the prediction obtained by only linearizing around the equilibrium position. Figure 5b and 5c show the estimated heave-heave frequency response function $\mathbf{K}_{3,3}(\omega)$ and the poles of the estimated state-space models for the re-linearization instances. The gradual shifting of the $\mathbf{K}_{3,3}(\omega)$ and poles as the platform moves indicates the variance of the dynamic characteristics of the fluid system.

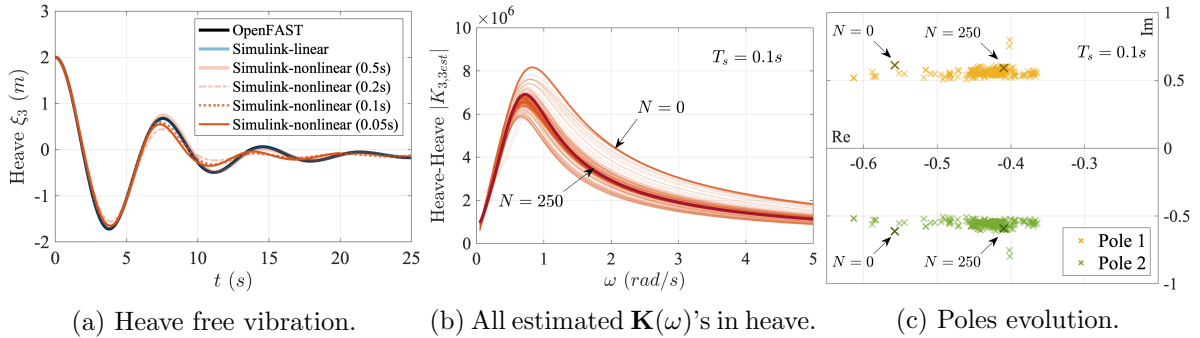


Figure 5: Platform heave free vibrations for different T_s , estimated frequency response function and poles of the fluid system for $T_s = 0.1s$.

5. Conclusions

A new piecewise re-linearization framework to evaluate the effects of body surface nonlinearity on the hydrodynamic behavior of FWTs is developed in this work. The framework utilizes hydrodynamic coefficients obtained from the open-source BEM code, Nemoh, at each operating point. The computationally efficient state-space representation is employed to approximate the fluid-memory radiation force. New features of data preprocessing and state-basis conversion are suggested to guarantee the robustness of the radiation force calculation. The implementation of this newly proposed re-linearization framework is studied in the Simulink model of a 5 MW ITIBarge FWT with rigid blades and tower. Free vibration tests are examined by releasing the FWT from an initial heave displacement, and the platform response simulated from the Simulink (pseudo) nonlinear model with re-linearization every T_s are compared against the linear model which only linearizes around the equilibrium. The results show that the Simulink nonlinear

model successfully captures the nonlinear effects of varying platform motions in a fast and robust manner, making it a promising tool for hydrodynamics calculation in the early design phases of FWTs. Future work will focus on investigating an adaptive re-linearization algorithm and implementing the piecewise linearization framework for general 3D platform movements of operating FWTs.

References

- [1] DNVGL-RP-0286 2019 Coupled analysis of floating wind turbines Standard DNVGL
- [2] Stehly T and Duffy P 2022 2021 cost of wind energy review Tech. rep. National Renewable Energy Lab.(NREL), Golden, CO, US
- [3] Openfast documentation, version v3.4.1 <https://openfast.readthedocs.io/en/main/> accessed: 2023-3-10
- [4] Hawc2 info <https://www.hawc2.dk/hawc2-info> accessed: 2023-3-10
- [5] Robertson A N, Wendt F, Jonkman J M, Popko W, Dagher H, Gueydon S, Qvist J, Vittori F, Azcona J, Uzunoglu E *et al.* 2017 *Energy Procedia* **137** 38–57
- [6] Li H and Bachynski-Polić E E 2021 *Ocean Engineering* **232** 109130
- [7] Leble V and Barakos G 2016 *Journal of Fluids and Structures* **62** 272–293
- [8] Yu Z, Ma Q, Zheng X, Liao K, Sun H and Khayyer A 2023 *Ocean Engineering* **268** 113050
- [9] Tran T T and Kim D H 2018 *Wind Energy* **21** 70–85
- [10] Nematbakhsh A, Olinger D J and Tryggvason G 2014 *Journal of Renewable and Sustainable Energy* **6** 033121
- [11] Tang S, Sweetman B and Gao J 2021 *Ocean Engineering* **229** 108866
- [12] Cottura L, Caradonna R, Ghigo A, Novo R, Bracco G and Mattiazzo G 2021 *Energies* **14** 248
- [13] Subbulakshmi A, Verma M, Keerthana M, Sasmal S, Harikrishna P and Kapuria S 2022 *Renewable and Sustainable Energy Reviews* **164** 112525
- [14] Giorgi G, Sirigu S, Bonfanti M, Bracco G and Mattiazzo G 2021 *Journal of Ocean Engineering and Marine Energy* **7** 439–457
- [15] Al-Solihat M K and Nahon M 2018 *International Journal of Mechanical Sciences* **142** 518–529
- [16] Chan G K Y, Sclavounos P D, Jonkman J and Hayman G 2015 *International Conference on Offshore Mechanics and Arctic Engineering* vol 56574 (American Society of Mechanical Engineers) p V009T09A038
- [17] Schubert B W, Robertson W S, Cazzolato B S and Ghayesh M H 2020 *Ocean Engineering* **197** 106828
- [18] Nemoh <https://gitlab.com/lheea/Nemoh> accessed: 2023-3-10
- [19] Cummins W, Iiuhl W and Uinm A 1962 *David Taylor Model Basin Washington DC*
- [20] McKelvey T, Akçay H and Ljung L 1996 *IEEE Transactions on Automatic control* **41** 960–979
- [21] Chatzis M N, Chatzi E N and Smyth A W 2015 *Earthquake Engineering & Structural Dynamics* **44** 523–547
- [22] Meng J, McAdam R A and Chatzis M N 2023 *Proceedings of the 41st IMAC, A Conference and Exposition on Structural Dynamics 2023, Austin, US*
- [23] Jonkman J M 2007 *Dynamics modeling and loads analysis of an offshore floating wind turbine* Ph.D. thesis University of Colorado at Boulder
- [24] Map++ <https://www.nrel.gov/wind/nwtc/map-plus-plus.html> accessed: 2023-3-10